JOURNAL OF GEOPHYSICAL RESEARCH, VOL. 104, NO. C6, PAGES 13,681–13,695, JUNE 15, 1999

Sensitivity of a global coupled ocean-sea ice model to the parameterization of vertical mixing

H. Goosse, E. Deleersnijder, and T. Fichefet

Institut d'Astronomie et de Géophysique G. Lemaître, Université Catholique de Louvain, Louvain-la-Neuve, Belgium

M. H. England

Centre for Environmental Modelling and Prediction (CEMAP), School of Mathematics, University of New South Wales, Sydney, Australia

Abstract. Three numerical experiments have been carried out with a global coupled ice-ocean model to investigate its sensitivity to the treatment of vertical mixing in the upper ocean. In the first experiment, a widely used fixed profile of vertical diffusivity and viscosity is imposed, with large values in the upper 50 m to crudely represent wind-driven mixing. In the second experiment, the eddy coefficients are functions of the Richardson number, and, in the third case, a relatively sophisticated parameterization, based on the turbulence closure scheme of Mellor and Yamada version 2.5, is introduced. We monitor the way the different mixing schemes affect the simulated ocean ventilation, water mass properties, and sea ice distributions. CFC uptake is also diagnosed in the model experiments. The simulation of the mixed layer depth is improved in the experiment which includes the sophisticated turbulence closure scheme. This results in a good representation of the upper ocean thermohaline structure and in heat exchange with the atmosphere within the range of current estimates. However, the error in heat flux in the experiment with simple fixed vertical mixing coefficients can be as high as 50 W m^{-2} in zonal mean during summer. Using CFC tracers allows us to demonstrate that the ventilation of the deep ocean is not significantly influenced by the paramertization of vertical mixing in the upper ocean. The only exception is the Southern Ocean. There, the ventilation is too strong in all three experiments. However, modifications of the vertical diffusivity and, surprisingly, the vertical viscosity significantly affect the stability of the water column in this region through their influence on upper ocean salinity, resulting in a more realistic Southern Ocean circulation. The turbulence scheme also results in an improved simulation of Antarctic sea ice coverage. This is due to to a better simulation of the mixed layer depth and thus of heat exchanges between ice and ocean. The large-scale mean summer ice-ocean heat flux can vary by more than 15% between the three experiments. Because of this influence of vertical mixing on Southern Ocean ventilation, sea ice extent, and ocean-atmosphere heat fluxes, we recommend that global climate models adopt a sufficiently realistic representation of vertical mixing in the ocean.

1. Introduction

The structure of the upper ocean is of paramount importance for atmosphere-ocean and ice-ocean exchanges. Because of the high heat capacity of water, the upper ocean acts as a huge heat reservoir which stores on the seasonal timescale about 5 times the atmospheric amount [*Oort and Vonder Haar*, 1976]. Any change in the seasonal cycle of the mixed layer depth modifies this storage, and thus influences ice-ocean fluxes. The mixed layer depth has also a direct impact on the evolution of the sea surface temperature (SST) because it controls the "effective" thermal inertia of the water column: When the mixed layer is deeper, the amount of fluid whose temperature has to be modified in a relatively short timescale is higher, and the variation of SST tends to be smaller for the same surface heat flux. As the SST is a key variable for the ocean-atmosphere heat flux, such a modification of the SST can in turn have strong consequences on the flux. In addition, mixing plays a role in the ocean dynamics by vertically redistributing the momentum and modifying the vertical profile of velocity [*Blanke and Delecluse*, 1993; *Johnson and Luther*, 1994].

The crucial role of mixing in the upper oceanic layers is clearly seen in coupled ocean-atmosphere models, which can be quite sensitive to the way this process is parameterized. For example, *Latif et al.* [1993] argued that the too warm SST in the summer hemisphere in their experiment can probably be attributed to too weak a surface mixing during summer months (and thus too weak a downward heat transport). In some other numerical experiments, *Latif et al.* [1994] showed that a bad representation of the surface mixing can cause an "unrealistic warm state within a relatively short time."

Nevertheless, because of their coarse vertical resolution, ocean general circulation models (OGCMs) used in climate studies do not often include an explicit representation of the evolution of the mixed layer depth [e.g., *Bryan and Lewis*, 1979; *Manabe and Stouffer*, 1994; *Hirst and Cai*, 1994; *Cubasch et al.*, 1995; *Washington and Meehl*, 1996]: They simply assume that the top oceanic level (generally of the

Paper number 1999JC900099.
0148-0227/99/1999JC900099$09.00

order of 20-50 m) can be considered as an implicit mixed layer of fixed depth. The only way to induce deeper mixing (apart from the effect of the small background vertical diffusivity) is through a convective adjustment scheme which is activated in case of unstable stratification. Thus the wind-driven mixing is ignored below the surface level. Even with higher vertical resolution, the mixed layer depth is sometimes considered to be a constant. In these studies, the vertical difusivity and viscosity can be increased between the top levels to take into account the effect of surface mixing [e.g., *Hirst and McDougall*, 1996]. However, this is a crude parameterization since the effectiveness of mixing varies very strongly with time and location. A more suitable method is to determine the vertical diffusivity and viscosity as functions of some local variables, related to processes which govern the intensity of mixing. For example, *Pacanowski and Philander* [1981] proposed expressions for vertical viscosity and diffusivity in which the role of stratification and velocity shear is taken into account through the Richardson number (see section 3).

Relatively complex turbulence models have also been introduced into OGCMs. Two kinds of such turbulence models are commonly used (see, for example, the recent review of *Large et al.* [1994]). The first type represents the mixed layer as a slab of thickness h with perfectly homogenous properties. The depth of the mixed layer is usually computed from the integral budget of turbulent kinetic energy. Such a model was used by *Sterl and Kattenberg* [1994] and *Williams et al.* [1995]. The second group relies on local, Fickian parameterizations of the turbulent fluxes in which eddy coefficients are necessary. The latter are computed from turbulent quantities derived from one or two differential equations [e.g., *Rosati and Miyakoda*, 1988; *Blanke and Delecluse*, 1993]. Very recently, *Large et al.* [1997] successfully used the new "K profile parameterization" (KPP) proposed by *Large et al.* [1994] in which the vertical diffusiviy is assumed to follow a nondimensional shape function. An additional term is also included in this parameterization to take into account the effect of nonlocal transport (i.e., not proportional to local gradients) under unstable forcing.

The major improvements brought by these sophisticated turbulence closure schemes are linked with a better representation of the temporal and spatial distribution of the mixed layer depth [*Rosati and Miyakoda*, 1988; *Blanke and Delecluse*, 1993; *Sterl and Kattenberg*, 1994; *Large et al.*, 1997]. This induces a temperature and salinity structure of the upper ocean in better agreement with observations as well as an improvement of the heat exchanges between ocean and atmosphere. In addition, the vertical velocity shear is better represented, particularly in equatorial regions, with implications on the intensity of the equatorial meridional cells or the equatorial undercurrent [*Blanke and Delecluse*, 1993]. However, *Large et al.* [1997] found only a minor impact of these parameterizations on deeper levels. The other studies cannot be used to draw conclusions at these deeper layers because of the short integration times.

Isopycnal models use a different type of mixing based on entrainment-detrainment across layer interfaces [*Hurlburt and Thomson*, 1980; *Bleck and Smith*, 1990; *Oberhüber*, 1993]. As a consequence, a comparison with the studies mentioned above, which all used z level models, is difficult and will not be performed here. In such models, the first isopycnal layer generally represents the mixed layer, whose evolution can be computed from an integral budget of turbulent kinetic energy, as in z level models (see above).

In the present paper, we analyze the role of vertical mixing in the upper ocean by comparing the results of three 750-year-long experiments performed with a global ice-ocean model (Table 1). In the first one, the diffusivity and viscosity are assumed to follow a prescribed profile. In the second one, the parameterization of *Pacanowski and Philander* [1981] is used, while the third experiment includes a turbulence closure scheme based on a simplified version of the Mellor and Yamada level 2.5 model [*Mellor and Yamada*, 1982; *Kantha and Clayson*, 1994]. Our goal is to investigate the implications of using schemes of different complexity to compute vertical mixing in OGCMs as well as studying the influence of vertical mixing in the ocean. Unlike previous studies, a sea ice model is explicitly coupled to the ocean. Thus our attention will be focused on polar regions (particularly the Southern Ocean). In addition, the use of CFCs as passive tracers, for the first time in such kind of numerical experiments, will provide information about the influence of vertical mixing in the upper ocean on the ventilation of the deep ocean which are complementary to the work of *Large et al.* [1997]. The analysis of the sensitivity of the model to vertical mixing in the deep ocean or to the use of diapycnal/isopycnal mixing tensor will not be performed. Even if various studies clearly demonstrate the influence of these parameterizations on the oceanic circulation and deep water properties [e.g., *Bryan*, 1987; *Hirst and Cai*, 1994; *England et al.*, 1994], this is out of the scope of the present work.

2. Description of the Ice-Ocean Model

Apart from the representation of vertical mixing, the version of the coupled large-scale ice-ocean (CLIO) model we use is similar to that referred to by *Goosse et al.* [1997a,b]. The model comprises a global, free-surface OGCM [*Deleersnijder and Campin*, 1995] coupled to a comprehensive sea ice model [*Fichefet and Morales Maqueda*, 1997]. The OGCM is a primitive equation model adopting the usual set of assumptions, i.e., the hydrostatic equilibrium and the Boussinesq approximation [e.g., *Bryan*, 1969]. The effect of mesoscale eddies is parameterized by a horizontal diffusion scheme, with horizontal eddy diffusivity and viscosity equal to 150 $m^2 s^{-1}$ and 10^5 $m^2 s^{-1}$, respectively. The sea ice model

Table 1. List of Experiments

Abbreviation	Parameterization of Vertical Mixing
CON	Fixed profile with high diffusivities and viscosities over the top 50 m
RI	Diffusivities and viscosities function of Richardson number (PP81)
TUR	Turbulence closure scheme based on Mellor and Yamada version 2.5

has a representation of both thermodynamic and dynamic processes. A three-layer model, which takes into account sensible and latent heat storage in the snow-ice system, simulates the changes of snow and ice thickness in response to surface and bottom heat fluxes. The variation of ice compactness due to thermal processes is a function of the energy balance of the surface layer in the region occupied by leads [*Fichefet and Morales Maqueda*, 1997]. For calculating ice dynamics, sea ice is considered to behave as a viscous-plastic continuum [*Hibler*, 1979].

At the ice-ocean interface, the sensible heat flux is proportional to the temperature difference between the surface layer and its freezing point and to the friction velocity (the square root of the ice-ocean stress divided by the water density), following the parameterization of *McPhee* [1992]. The ice-ocean stress is taken to be a quadratic function of the relative velocity between ice and the uppermost level of the ocean (depth =5 m), with a drag coefficient of 5×10^{-3}. Considering salt and freshwater exchanges between ice and ocean, brine is released to the ocean when ice is formed, while freshwater is transferred to the ocean when sea ice or snow melts. The sea ice salinity is assumed to be constant (4 psu). For more details about the coupling technique, see *Goosse* [1997] or *Fichefet et al.* [1998]

The governing equations of the model are solved numerically by using a finite volume technique on an Arakawa B grid. The horizontal resolution is 3°×3°. In order to avoid the North Pole singularity, two spherical grids are patched together. The first one is a standard geographical latitude-longitude grid covering the whole world ocean, except for the North Atlantic and the Arctic which are represented in a spherical coordinate system having its poles on the equator. The two grids are connected to each other in the equatorial Atlantic [*Deleersnijder et al.*, 1993]. The water flow through Bering Strait is parameterized as a linear function of the cross-strait sea level difference in accordance with the geostrophic control theory [*Goosse et al.*, 1997a]. The so-called "z coordinate" underlies the vertical discretization, with 20 levels ranging in thickness from 10 m at the surface to 750 m in the deep ocean, with 6 levels in the top 100 m. Close to the surface, the vertical resolution is higher than that commonly used in OGCMs: This is believed to be necessary to ensure appropriate representation of surface processes and a proper functioning of the turbulence closure model. However, it must be realized, however, that having six levels in the top 100 m represents a relatively coarse resolution compared to some models using a similar turbulence scheme in smaller-scale studies [e.g., *Oey and Mellor*, 1993; *Kantha and Clayson*, 1994].

The model is driven by surface fluxes of heat, freshwater, and momentum determined from the empirical bulk formulae described by *Goosse* [1997]. Input fields consist of monthly climatological surface air temperatures [*Taljaard et al.*, 1969; *Crutcher and Meserve*, 1970], cloud fractions [*Berliand and Strokina*, 1980], relative air humidities [*Trenberth et al.*, 1989], precipitation rates [*Jaeger*, 1976], and surface winds and wind stresses from *Hellerman and Rosenstein* [1983] between 15°S and 15°N and from *Trenberth et al.* [1989] out of this latitude band. The river runoffs are based on the annual mean climatology of *Baumgartner and Reichel* [1975]. Owing to inaccuracies in the precipitation and runoff data and in the evaporation computed by the model, the net freshwater flux at the surface exhibits a slight imbalance inducing a drift in the simulated global salinity. To remedy this problem, a weak relaxation to annual mean observed salinities [*Levitus*, 1982] is applied in the surface layer with a time constant of 60 days. To give an order of magnitude, this restoring induces a freshwater flux equivalent to 18 cm of water per year if the difference between the simulated salinity and Levitus data is equal to 0.1 psu.

The flux of CFC-11 at the ocean-atmosphere interface is computed as in the most comprehensive parameterization of *England et al.* [1994] (CF4). The gas flux is proportional to the difference between the CFC concentration in the ocean and the saturation concentration in equilibrium with the atmospheric value, which is deduced from observational estimates for the period 1930-1994. The coefficient of proportionality (gas piston velocity) depends on the wind speed and on the Schmidt number [*Wanninkof*, 1992]. In addition, the CFC flux in polar regions is reduced according to the fractional sea ice coverage in the grid box to take into account the shielding effect of the ice cover. In the ocean interior, CFC behaves as a passive tracer.

3. Parameterization of Vertical Mixing

In the first experiment, the vertical diffusivity and viscosity K_S and K_u follow a prescribed profile (hereafter termed CON) (Table 1). High values of the eddy coefficients ($K_S = K_u = 2 \times 10^{-3}$ m^2 s^{-1}) are applied in the top 50 m to simulate a 50 m deep mixed layer. Below this layer, the vertical diffusivity follows the classical profile of *Bryan and Lewis* [1979] (Figure 1) and the viscosity is constant ($K_u = 10^{-4}$ m^2 s^{-1}). Thus this experiment is directly comparable to similar cases studied by *England et al.* [1994] or *Hirst and Cai* [1994].

In the second experiment (hereafter termed RI), the vertical diffusivity and viscosity are functions of the Richardson number (Ri) defined as

$$Ri = \frac{N^2}{M^2} \tag{1}$$

with

$$\left(N^2, M^2\right) = \left(-\frac{g}{\rho_0}\frac{\partial \rho}{\partial z}, \left|\frac{\partial U}{\partial z}\right|^2 \right) \tag{2}$$

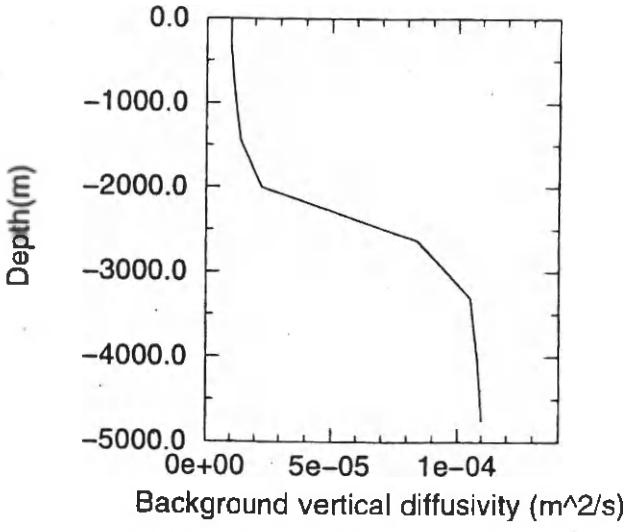

Figure 1. Vertical profile of the model background vertical diffusivity in m^2 s^{-1}.

where g is the gravitation acceleration, ρ_0 is the reference density, ρ is the water density, z is the vertical coordinate, and U is the horizontal velocity vector.

A slightly modified *Pacanowski and Philander* [1981] (hereafter PP81) parameterization is used:

$$K_u = \frac{K_{u0}}{(1+\alpha Ri)^n} + K_{ub} \tag{3}$$

$$K_s = \frac{K_{s0}}{(1+\alpha Ri)^{n+1}} + K_{sb} \tag{4}$$

where K_{sb} and K_{ub} are the background diffusivity and viscosity, respectively, which take values identical to those used in experiment CON below the surface layer (Figure 1); α and n are two constants equal to 5 and 2, respectively (PP81). PP81 used constant values for the parameters K_{s0} and K_{u0}. As the parameterization in its classical form tends to underestimate turbulent mixing close to the surface, *Campin* [1997] has proposed to increase K_{s0} and K_{u0} in the upper ocean. The values used here decrease from 10^{-1} m^2 s^{-1} at the surface to 10^{-2} m^2 s^{-1} at 50 m (the value proposed by PP81) and then remain constant. Minimum values for mixing at the surface are also prescribed as by *Philander and Pacanowski* [1986] : $K_u = 10^{-3}$ m^2 s^{-1} and $K_s = 3 \times 10^{-5}$ m^2 s^{-1}. This parameterization was used in a former version of the model and experiment RI is identical to the experiment OP of *Goosse et al.* [1997b].

In the third experiment (hereafter termed TUR), a more sophisticated representation of vertical mixing has been introduced in CLIO based on a simplified verion of the Mellor and Yamada level 2.5 model [*Mellor and Yamada*, 1982; *Kantha and Clayson*, 1994]. The vertical viscosity and diffusivity are taken to be proportional to the characteristic velocity (q) and length (l) of turbulent motions:

$$K_u = l\, q\, S_u \tag{5}$$

$$K_s = l\, q\, S_s \tag{6}$$

where S_u and S_S are stability functions calculated according to *Kantha and Clayson* [1994], who provided a complete description of these terms.

Let q denote the turbulent velocity scale. Then the budget of turbulent kinetic energy, q^2, reads [*Mellor and Yamada*, 1974, 1982]

$$\frac{Dq^2}{Dt} = 2K_u M^2 - 2K_s N^2 - \frac{2q^3}{B_1 l} + \frac{\partial}{\partial z}\left(K_q \frac{\partial q^2}{\partial z}\right) \tag{7}$$

where B_1 is a constant equal to 16.6 and K_q is the coefficient of diffusion of q^2 given by an expression similar to (5).

It is now necessary to specify the turbulence macroscale l, which is the characteristic size of the energy-containing eddies. The Mellor and Yamada level 2.5 model classically solves an additional differential equation for the product $q^2 l$, which is then used to deduce l, knowing q^2 from (7). Here, for simplicity, l is prescribed as an algebraic function:

$$l = l_0 \frac{k\, L_d}{k\, L_d + l_0} \tag{8}$$

where

$$L_d = \frac{d_s\, d_b}{d_s + d_b} \tag{9}$$

Here d_s and d_b are the distances to the surface and the bottom, respectively, k is the von Karman constant (0.4), and l_0 is a constant (10 m).

An additional constraint is imposed on l to avoid unphysical results [*Kantha and Clayson*, 1994]:

$$l \le C_4 \frac{q}{N} \tag{10}$$

with C_4 equal to 0.53. It must be stressed that the value of l given by (8) is generally much larger than the limit provided by (10). As a consequence, (8) only applies in slightly stratified regions.

The scheme described above is valid only in fully turbulent regions like the surface mixed layer. Another parameterization is needed in the regions below, where the turbulence tends to be intermittent. For the strongly stable and strongly sheared region immediately below the mixed layer, we again follow *Kantha and Clayson* [1994] who used the parameterization proposed by *Large et al.* [1994]. For deeper layers, a minimum background viscosity and diffusivity are imposed (Figure 1), with the same values as in experiments CON (below the surface layer) and RI.

In all three experiments, the vertical diffusivity is increased to 10 m^2 s^{-1} whenever the density profile is statically unstable, in order to remove gravitational instabilities. The model is not sensitive to this value provided that it is sufficently large. This increase of vertical diffusivity in case of unstable stratification is absolutely necessary in experiments CON and RI to avoid unphysical results. Besides, an experiment similar to TUR but without such an increase has shown that it has only a moderate impact on the characteristics of the simulation [*Goosse*, 1997]. In this experiment, the turbulence scheme is able to simulate reasonably well deep mixing even if relatively strong static instabilities remain at some locations. Anyway, the increase of diffusivity in unstable regions has been maintained in TUR so that differences between experiment CON, RI, and TUR cannot be attributed to a different treatment of unstable water columns.

It must be stressed that the three mixing schemes are responsible for a relatively small fraction of the total CPU time consumption of the model. Therefore a choice between the schemes cannot be justified on the basis of a significant computer time difference only. On our Convex 3820, about 45% of the CPU time is devoted to the computation of the surface forcing and of the evolution of the ice characteristics. The remaining time is mainly due to the computation of ocean velocity, temperature, and salinity. The routines dealing with vertical mixing in CON and RI execute relatively simple operations and so consume only about 1% of the total CPU amount. The operations are more complex in TUR, but this part of the code is still cheaper than, for example, the computation of ocean temperature since it does not include the costly three-dimensional (3-D) advection scheme. As a consequence, the relative CPU consumption of vertical mixing in TUR is of about 3% of the total.

4. Results and Discussion

4.1. Mixed Layer Depths

The mixed layer depth (MLD), defined as the depth where the potential density exceeds by 0.125 kg m^{-3} the surface value (as given by *Levitus* [1982]), is displayed in zonal mean

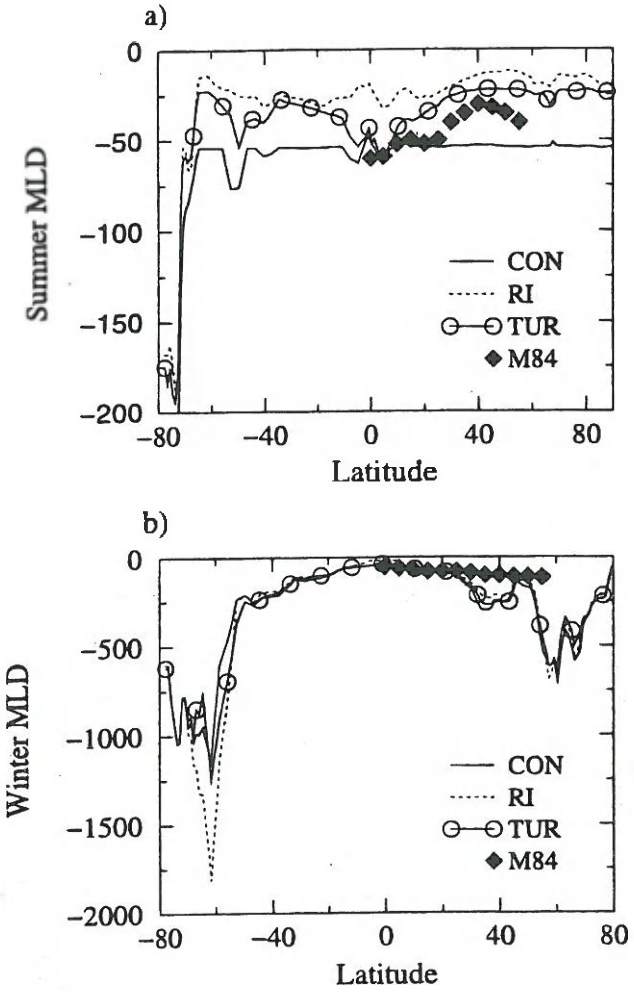

Figure 2. Zonally averaged mixed layer depth for the global ocean in summer (monthly mean for September in the Northern Hemisphere and March in the Southern Hemisphere) and in winter (March in the Northern Hemisphere and September in the Southern Hemisphere). Experiment CON is represented by a solid line, experiment RI is represented by a dashed line, experiment TUR is represented by a solid line with circles, and the estimates of *Meehl* [1984] are represented by diamonds.

for the three experiments in Figure 2. At the end of summer, the mixed layer in CON is close to 50 m everywhere, except near Antarctica where sea ice formation has already begun at this time. This tends to destabilize the water column and generate deep mixed layers. Close to Antarctica, the shallowest mixed layer (about 50 m) occurs in January-February, when ice melting is responsible for a retreat of the mixed layer. A summer MLD of 50 m seems more or less reasonable in most of the ocean, but it is generally too deep poleward of 30°. For example, a zonal mean of 30 m in the latitude band 30°-50°N is probably more reasonable during this season [*Bathen*, 1972; *Levitus*, 1982; *Lamb*, 1984; *Meehl*, 1984]. In experiment RI, the mixed layer depth displays interesting meridional variations, but the mixed layer is too shallow, with depths rarely greater than 30 m. The mixing due to the PP81 parameterization, even with the modifications introduced for the purposes of the study (see section 3), is too weak, which is in agreement with *Blanke and Delecluse* [1993] and *Sterl and Kattenberg* [1994]. In experiment TUR, the observed meridional structure of the MLD is well reproduced with values around 50 m at the equator which decrease toward the midlatitudes [*Lamb*, 1984; *Meehl*, 1984]. Nevertheless, the mixed layer appears to be still too shallow but much less so than in RI.

In winter, the mixed layer is deeper than in summer because of the destabilizing effect of the surface buoyancy flux. Whenever this flux tends to induce an unstable stratification, the water column is mixed to a depth such that the static stability is restored. This process is represented in the same way in all experiments, i.e., by the convective adjustment scheme. As a consequence, the simulated winter MLDs are close to each other. Differences of a few meters to tens of meters are noticed, but this is generally a few percent of the mixed layer depth itself. In all the experiments, the observed meridional distribution is relatively well simulated with shallow mixed layers in tropical regions, a deepening in the subtropical gyre with a local maximum at about 40°N and a shallowing a little northward. The deep zonal mean in the high latitudes of the Northern Hemisphere is a consequence of the deep convection in the Labrador Sea and in the Greenland-Iceland-Norwegian (GIN) seas, which can reach more than 2000 m in the model. The local maximum at about 40°N is not present in the estimates of *Meehl* [1984] but can be noticed in some other data sets [e.g., *Levitus*, 1982; *Lamb*, 1984]. The Southern Ocean is the only region where the differences between the experiments are significant in this season. The mixed layers there are very deep during winter. It is probably a little overestimated in Figure 2 because the definition used for the MLD is not well adapted in these weakly stratified areas. Nevertheless, the comparison of CFC concentration simulated by the model with observations shows that the ventilation in the Southern Ocean is overestimated in all the simulations (see section 4.4). This is a classical problem of models using a simple horizontal diffusion scheme [e.g., *England and Hirst*, 1997]. The error is largest in experiment RI, in which the mixed layer is 500 m deeper at 60°S than in the other two experiments. A detailed analysis of this is made in sections 4.4 and 4.5.

4.2. Temperature Fields and Heat Fluxes

The horizontal and annual mean temperatures in the upper 100 m are very well simulated in experiment TUR (Figure 3), with a vertical profile very close to the observations of *Levitus* [1982]. In experiment CON, the deeper mixed layer in summer allows a more intense transfer of heat from the surface and a subsequent warming in the upper layer. As the winter mixed layer has nearly the same depth in CON and in TUR, the temperature differences are much smaller than in summer and the annual mean temperature difference reflects the summer value. This results in a mean temperature at 50 m in CON more than 1°C warmer than the Levitus data. However, the too shallow mixing in summer in RI is associated with too cold temperatures. The mean error on instantaneous temperature is also lower in experiment TUR, but the improvement is a little smaller. For instance, the horizontal mean of the difference between model and Levitus observations at 45 m is 1.07°C in TUR, 1.23°C in CON, and 1.34°C in RI, i.e., an improvement in TUR of about 15% compared to CON and 25% compared to RI. From 75-100 m toward the bottom, the profiles in the three experiments are nearly similar, the influence of the various parameterizations being smaller there. Nevertheless

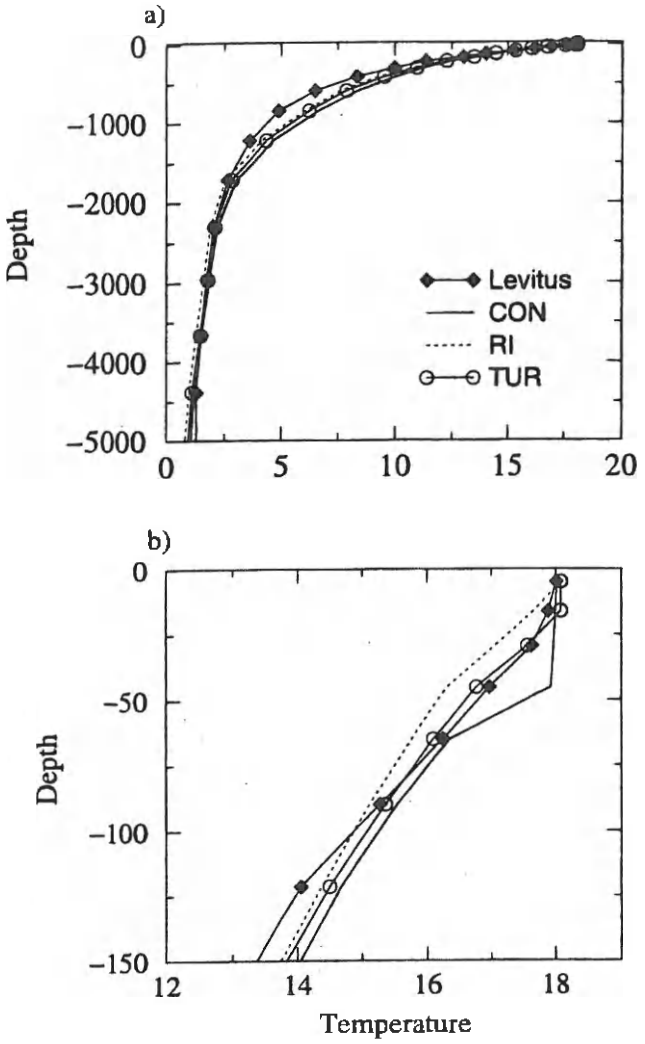

Figure 3. Horizontal average of the annual mean temperature in the global ocean (°C) for experiment CON (solid), RI (dashed), TUR (solid with circles), and *Levitus* [1982] observations (solid with diamonds).

experiment CON is still the warmest, and RI is the coldest (as in the surface layer). The agreement between the model and observations is good at greater depths in horizontal mean, except between 500 and 1500 m where the model is too warm and the thermocline is a little too diffuse. This is a classical problem of the type of OGCM used here. The results of our experiments suggest that it is not due to the parameterization of vertical mixing in the upper ocean.

These changes of the global mean vertical profile reflect well the variations in all the oceanic basins, except the Southern Ocean, as discussed in section 4.5. Indeed, when comparing the three experiments in a particular region (not shown), a general improvement of the model results in the surface layer in TUR is also found compared to RI and CON, and almost no difference is found below.

The annual mean SST hardly changes from one experiment to another (a maximun difference of 0.04°C on the horizontal mean) because the atmospheric variables are assumed to be independent of the simulated ocean. The SST is thus mainly determined by the forcing, the way the fluxes are computed being roughly equivalent to a restoring technique. However, the flux needed to obtain this SST strongly changes (Figure 4). The zonally averaged net surface heat flux simulated in experiment TUR corresponds quite well with estimates [*Hsiung*, 1986; *Da Silva et al.*, 1994], with, for example, a warming in summer which reaches 125 W m^{-2} at 45°N in June and a corresponding cooling in winter.

More detailed comparison of the various experiments with fluxes derived form observations is difficult because of the uncertainties in these estimates [e.g., *Da Silva et al.*, 1994]. In addition, the ocean-atmosphere heat flux is strongly dependent on the atmospheric data and on the parameterization used to compute the flux. To identify the influence of the parameterization of vertical mixing, it seems more interesting to compare the three experiments to each other, the way the forcing is computed remaining the same. Experiment TUR is assumed to be the reference because it has the best representation of MLD and of the vertical profile of temperature. Furthermore, the mean error of the zonally averaged heat flux compared to *Da Silva et al.* [1994] estimates is minimum in this case (13.6 W m^{-2} in TUR; 15.4 W m^{-2} in RI; 19.1 W m^{-2} in CON). Nevertheless, these values are probably not very significant since the accuracy of the heat flux of *Da Silva et al.* [1994] is probably not greater than +/- 10-20 W m^{-2}, the error being even stronger in high latitudes.

In experiment RI, as the summer mixed layer is shallower than in TUR, the fluxes needed to warm the mixed layer are smaller. This leads to an underestimation of the flux, the difference being as high as 25 W m^{-2} (Figure 4c). The lack of heat accumulation in summer leads to too small a transfer to the atmosphere in winter when the mixed layer deepens again, the difference in surface fluxes between the two experiments being of the same order in both seasons. The pattern is opposite in experiment CON in which the erroneously deep mixed layers are associated with much too intense heat flux from the atmosphere to the ocean in summer and too high a flux from the ocean to the atmosphere in autumn and winter (Figure 4d). The difference can be as high as 50 W m^{-2}, which is significantly higher than the uncertainties on the flux, demonstrating that the surface heat fluxes in this experiment are probably not satisfactory.

4.3. Ocean Velocities

The velocity field in the upper layers is affected by the modifications of vertical viscosity in the three experiments. The most direct consequence is on the magnitude of the surface velocity which is, on average, 30% higher in RI than in TUR, because of the weaker mixing. The surface velocity in CON is of the same magnitude as in RI but this, of course, depends on the value of the viscosity imposed in the top layer. The influence is also particularly strong in the equatorial regions. These processes have been analyzed thoroughly by *Blanke and Delecluse* [1993] for the Atlantic Ocean, so they are not repeated here. Nevertheless, it is worth mentioning that a strong reduction in equatorial upwelling is observed in the Atlantic in TUR (8 Sv), as was also noticed by *Blanke and Delecluse* [1993] when comparing experiments similar to TUR and RI. The equatorial upwelling in CON is relatively close to the one in RI. However, the differences of velocity in the deeper ocean are weak. For instance, the maximum of the meridional stream function in the Atlantic at 30°S (which can be considered as a measure of the North Atlantic Deep Water exported out of the basin) is 15.7 Sv in CON, 15.8 Sv in RI [*Goosse et al.*, 1997b], and 16.1 Sv in TUR.

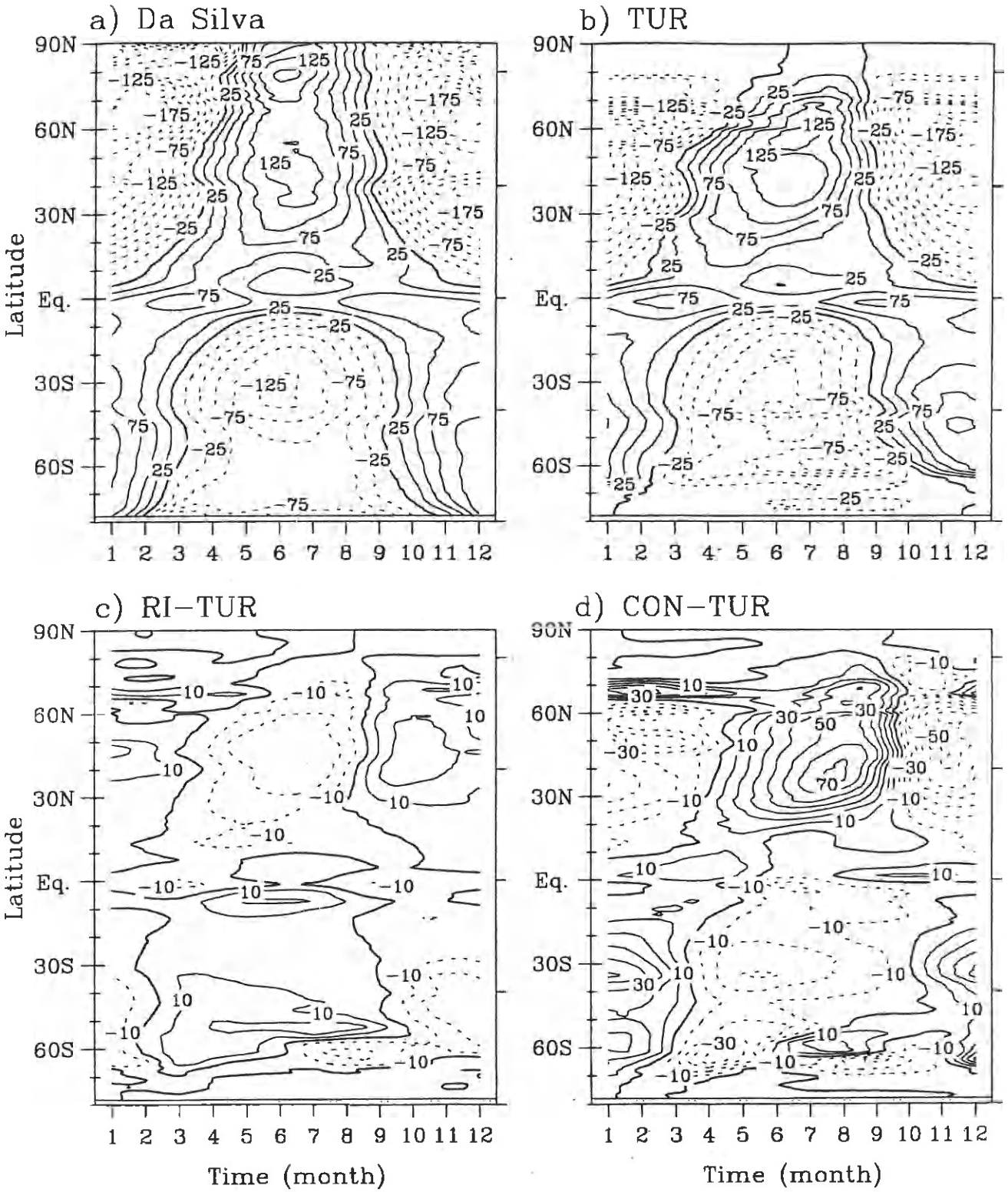

Figure 4. (a) Time evolution of the zonal mean surface heat flux of *Da Silva et al.* [1994]. (b) Same as Figure 4a, except for experiment TUR. (c) Same as Figure 4a for the difference of surface heat flux between experiments RI and TUR (RI-TUR). (d) Same as Figure 4a for the difference of surface heat flux between experiments CON and TUR (CON-TUR). Contour interval is 25 W m^{-2} for Figures 4a and 4b and 5 W m^{-2} for Figures 4c and 4d. Fluxes are considered positive downward (toward the ocean).

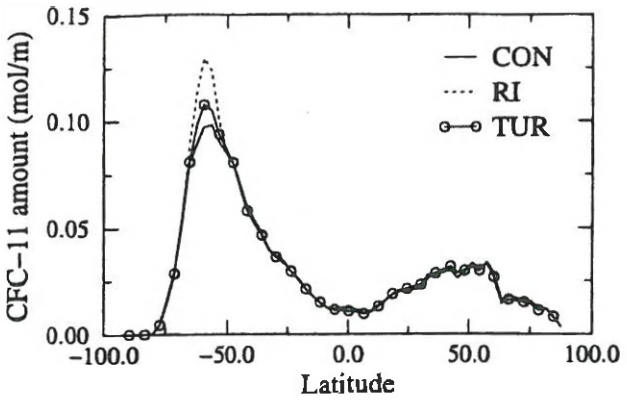

Figure 5. Total amount of CFC-11 in the ocean in 1994 per latitude band (in mol m^{-1}) in experiments CON (solid), RI (dashed), and TUR (solid with circles).

4.4. CFC Simulations

The simulated concentrations of CFC-11 in the ocean are mostly similar in the three experiments, as shown by the total oceanic content of CFC-11 in 1994 (Figure 5). The only exception is the Southern Ocean, where the shallower mixed layer in winter in experiments TUR and CON leads to a much weaker ocean ventilation than in RI. This results in a higher maximum of the zonally and vertically integrated amount of CFC-11 in RI (0.129 mol m^{-1}) than in TUR (0.107 mol m^{-1}) and CON (0.098 mol m^{-1}) (Figure 5). Global observations of CFC-11 are not densely sampled, so we cannot compare this figure with data. However, as already mentioned, the ventilation is overestimated in the Southern Ocean in all three simulations; so, the best results are probably those of CON. This is illustrated by the comparison with in situ measurements made at about 150°E during 1991 (World Ocean Circulation Experiment section SR3) with model results for

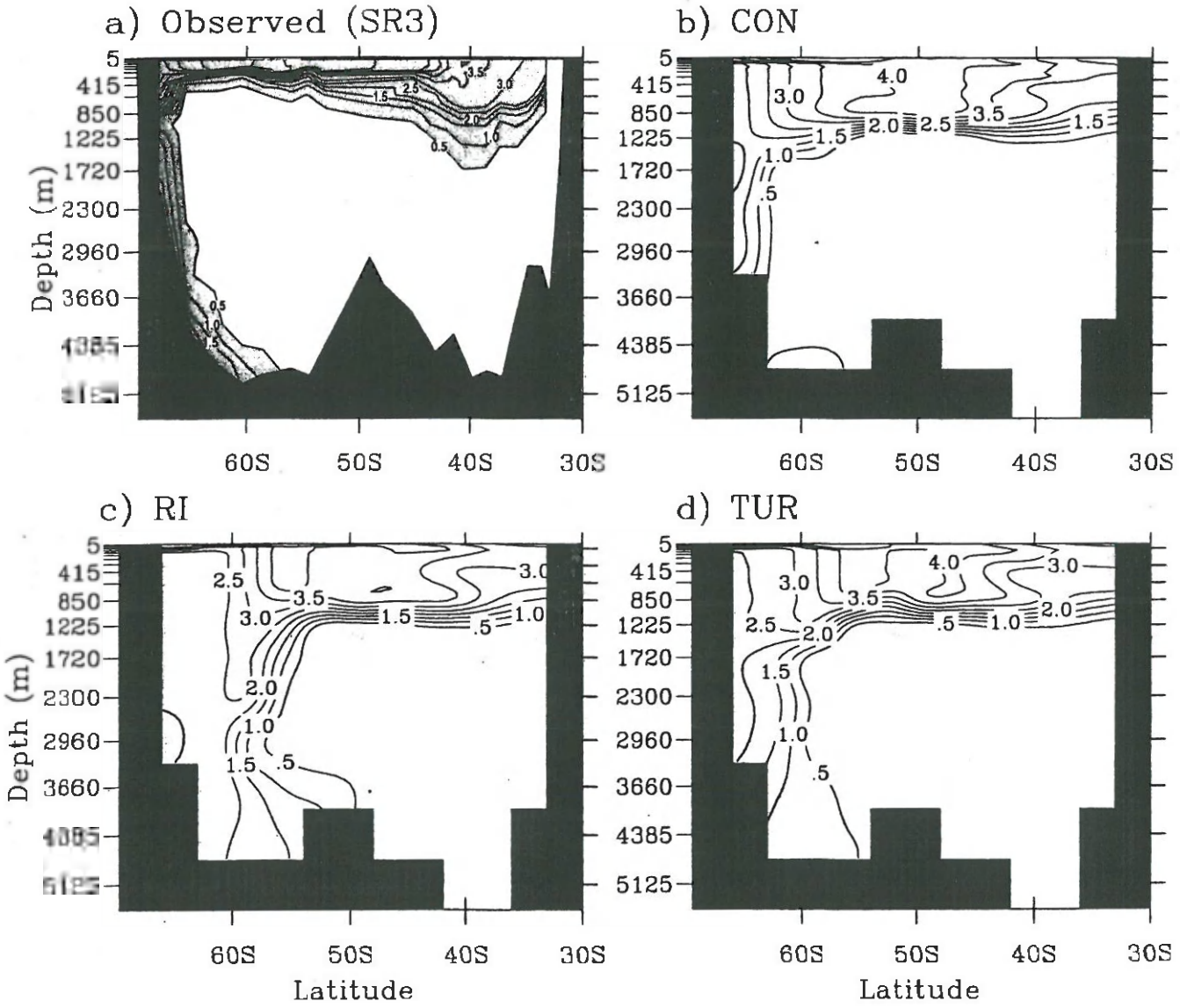

Figure 6. Section of CFC-11 in the Southern Ocean in 1991 at approximately 150°E. (a) Observed (data provided courtesy of J.L. Bullister, figure from *England and Hirst* [1997]). (b) Experiment CON. (c) Experiment RI. (d) Experiment TUR. Contour interval is 0.5 pmol kg^{-1}.

the same period (Figure 6). For instance, at 60°S, the concentrations higher than 2.5 pmol kg^{-1} are restricted to the upper 400 m in the observations, while such values are found up to 900 m in CON, 1300 m in TUR, and 2300 m in RI.

The similar amounts of CFC-11 in Figure 5 suggest that in most of the ocean (i.e., except the Southern Ocean), the ventilation of the thermocline and of the deep ocean are only weakly dependent on the parameterization of vertical mixing in the upper ocean. This is consistent with the weak modifications of temperature, salinity, and velocity we see at great depths and with the findings of *Large et al.* [1997]. This relative model insensitivity seems not difficult to understand. First, the vertical viscosity and diffusivity given by the three parameterizations are identical below the surface layer: They are equal to the background diffusivity or viscosity. As a consequence, there is no direct effect of the parameterization there. Nevertheless, as the water masses originate from the surface, the mixing modification in the upper layer might influence the ocean interior. In fact, this turns out not to be the case because deep water formation occurs during wintertime when MLD and mixed layer properties happen to be quite similar for all three parameterizations.

Stommel [1979] has argued that the subduction of water into the main thermocline occurs only at the end of winter when the MLD is at a maximum. The water subducted from the mixed layer base in summer has insufficient time to go deep enough before the winter deepening and is thus incorporated again into the mixed layer. However, a fraction of the late winter mixed layer is left at greater depths when the mixed layer retreats; this water can then escape the surface layer before the mixed layer reaches again its maximum in the following winter. This escape into the main thermocline is made by either downward advection and/or horizontal transport to a point where the mixed layer becomes shallower. As a consequence, the properties of the water in the main thermocline match those of the mixed layer in winter [*Iselin*, 1939]. The basic ideas of this mechanism have been confirmed by various studies based on data [e.g., *Qiu and Huang*, 1995] or by the analysis of model results [e.g., *Williams et al.*, 1995]. Stommel provides an image of this phenomenon as a demon which only allows a passage of mixed layer water during winter.

As stated above, the winter mixed layer depths and properties are nearly identical in our three experiments. As a consequence, the water which is transferred to the deeper layers has similar characteristics. This results in the small differences of temperature, salinity (and subsequently velocity), and CFC concentration noted above.

4.5. Role of Salinity and Freshwater Fluxes in the Southern Ocean

The MLD (Figure 2), CFC concentration (Figure 5), and salinity (Figure 7) changes between the three experiments in the Southern Ocean are a consequence of a relatively complex mechanism. In order to gain some insight into these processes, we calculated the annual mean freshwater balance of the top 25 m of the ocean southward of 55°S (Table 2 and Figure 8). In this computation, the freshwater flux at the surface includes precipitation and evaporation as well as the effect of the restoring term. The freshwater flux associated with exchanges between ice and ocean is also included but is very small when integrated over the relevant region, the various contributions cancelling each other. The second contribution to the budget, the horizontal transport at the northern boundary, is computed in the classical way:

$$F_s = \int_{-25}^{0} \int_{-180°}^{180°} \frac{v(\bar{S} - S)}{S} \, d\lambda \, dz \qquad (11)$$

where λ is longitude, v is the northward component of velocity, S is the local salinity, and $\bar{S}$ is a reference salinity. $\bar{S}$ is chosen to be 34.6 psu, which is close to the mean model salinity in the Southern Ocean. Finally, the vertical freshwater transport is due to vertical advection, diffusion, and convection and is equal to the difference between the two other terms, the 25 m layer being in equilibrium on annual mean.

The difference between the freshwater flux at the surface in the various experiments is a consequence of changes in the restoring term. This is because precipitation is identical in the three experiments and evaporation varies only weakly. In CON, the annual mean surface salinity is higher than in the other two experiments. The difference occurs mainly in summer, when the mixed layer is deeper than in TUR and RI (Figure 2). The surface freshwater input during this season is thus distributed over a greater depth than in TUR and RI, resulting in higher surface salinities and consequently higher restoring fluxes.

The changes of the lateral freshwater transport between the three experiments can be due to modifications of the salinity of the water exported or to the modification of the volume transport (11). In RI and CON, the values are similar because the effect of the lower salinity and mass transport in RI compared to CON compensate each other. In these two experiments, nearly the whole Ekman transport is achieved in the top 25 m (less than 3 Sv northward transport below 25 m). This is not the case in TUR; the higher vertical viscosities cause a significant part of the wind-induced northward volume transport to be between 25 and 60 m (8 Sv). As a result, the volume transport in the top 25 m is lower in TUR and so therefore is the horizontal freshwater flux.

The higher surface freshwater input in CON and the smaller horizontal freshwater transport in TUR is balanced by a 10% increase in the vertical transport at 25 m in these two experiments compared to RI. This induces a decrease of the salinity in the layer between 25 and 100 m in TUR and CON compared to RI (Figure 7); exactly in the same way as a higher precipitation rate in a particular region tends to decrease the surface salinity. As a consequence, the stability of the upper ocean compared to the deeper layer is higher in TUR and CON. This induces shallower winter mixed layers in these two experiments (Figure 2) and thus a lower ventilation rate in the Southern Ocean (Figure 5 and Figure 6).

Table 2 shows that the Southern Ocean freshening between 25 and 100 m in TUR is fundamentally a three-dimensional process in which the modification of the vertical distribution of velocity plays a crucial role. The decrease of the salinity in TUR compared to RI over the whole water column southward of 65°S (Figure 7) confirms this finding. This indeed cannot be due to a simple vertical mixing effect otherwise some regions of higher salinities would compensate for regions of lower salinities. Nevertheless, the vertical diffusion is important since it contributes to the downward transport of the freshwater "left" in the upper layer due to the smaller horizontal transport. Besides, the freshening in CON seems to be mainly associated with vertical processes. The higher vertical mixing rate generates a nonphysical increase of the

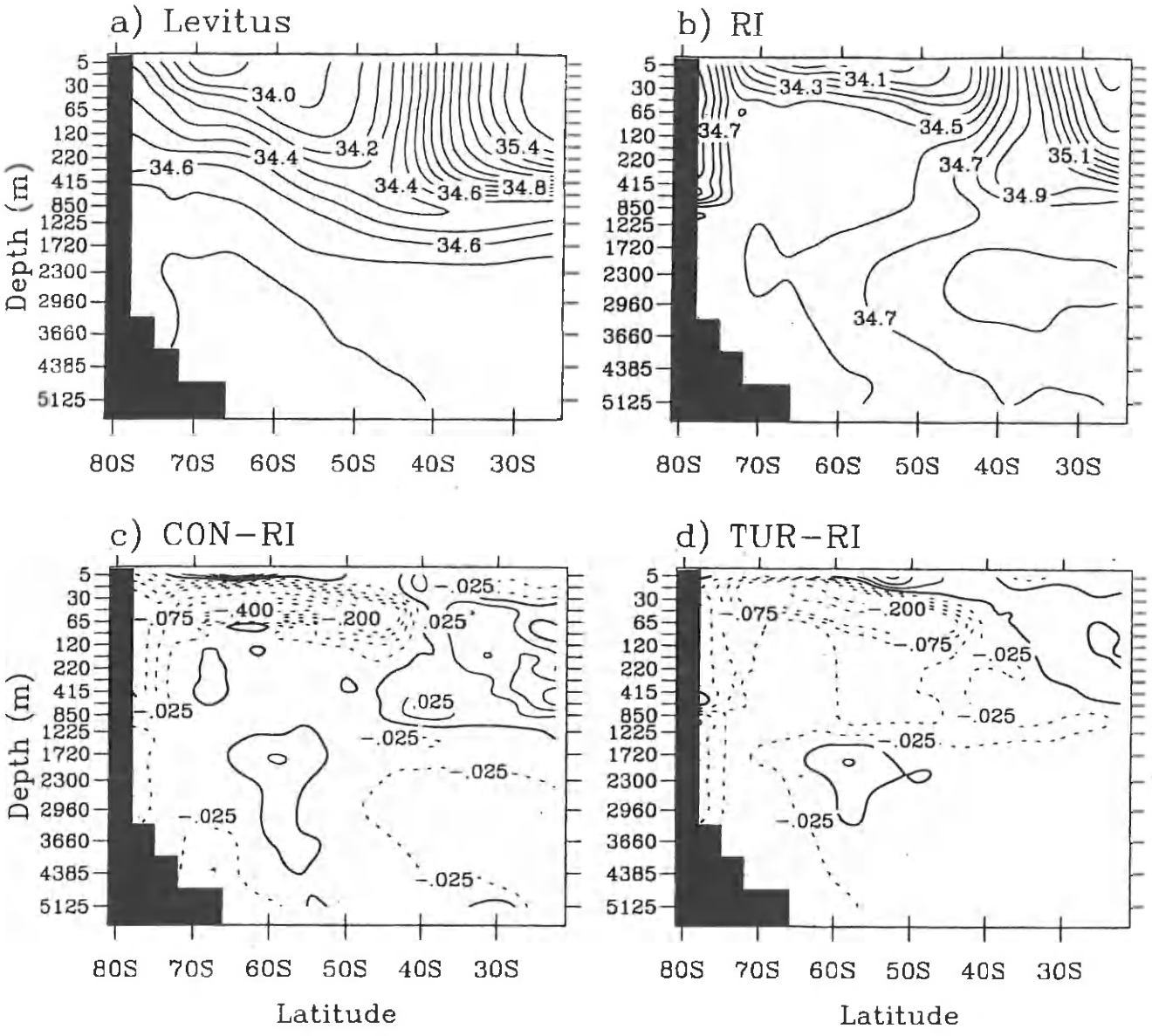

Figure 7. Zonal average of the annual mean salinity. (a) Observed [*Levitus*, 1982]. (b) Experiment RI. Contour interval is 0.1 psu. Zonal average of the difference of annual mean salinity (c) between CON and RI (CON-RI) and (d) between TUR and RI (TUR-RI). Contour interval is 0.025 psu between -0.1 psu and 0.1 psu and 0.1 psu out of this range.

surface flux and a transport of a significant part of this freshwater to depths below 25 m. However, it must be stressed that the higher vertical mixing in CON also tends to increase the surface salinity and thus to decrease the horizontal freshwater transport close to the surface (11). Without the restoring which constrains the surface salinity evolution, this effect would have likely been more important.

The decrease of salinity in the upper ocean in TUR and CON compared to RI induces a weak freshening of the water masses formed in the Southern Ocean. The effect on Antarctic Bottom Water (AABW) is apparent near Antarctica, close to the bottom, and a slight freshening of Antarctic Intermediate Water (AAIW) is noticed in TUR (Figure 7). However, the salinity in a zone centred at about 55°S, roughly between 1500 and 3000 m is higher in CON and TUR than in RI (Figure 7). This part of the ocean in RI is in direct contact with the fresh surface waters. This it is not the case in TUR and CON because of the shallower mixed layers, resulting in a salinity increase in these two experiments. The slower oceanic ventilation in TUR and CON also induces an oceanic warming at depth because of the lower exchanges with the cold atmosphere (not shown). The maximum of the temperature differences below the surface level is located at about 1500 m and reaches 0.4°C in TUR and 0.6°C in CON (compared to RI). The changes in TUR and CON improve the results of our simulation, but they do not totally cure the systematic bias in the model Southern Ocean. For example, the upper ocean and AAIW are still too salty by about 0.2-0.3 psu in TUR and the

Table 2. Annual Mean Freshwater Balance of the Top 25 m of the Ocean Between 55°S and Antarctica in The Three Experiments

Experiment	Surface input	Lateral Freshwater *Transport*	Vertical Freshwater *Transport*	Northward Mass *Transport*
CON	0.56	0.32	0.24	24.6
RI	0.60	0.33	0.27	26.3
TUR	0.55	0.28	0.27	19.9

The balance is in Sv of freshwater. In addition to the freshwater fluxes, the northward mass transport at 55°S in the top 25 m has been added (in Sv).

Southern Ocean below 1000 m is too cold and fresh (Figure 9). This latter problem is mainly due to erroneously strong mixing there, both in TUR and CON (Figure 6).

4.6. Ice Coverages

The different mixing parameterizations lead to substantially different ice coverages (Figure 10 and 11). In winter, the Antarctic ice extent obtained in the various experiments is influenced by changes in mixed layer depth in the Southern Ocean. The major differences occur in the Indian sector between 30° and 90°E. In RI, the too deep mixed layer brings relatively warm deep water to the surface, resulting in a significant underestimation of the ice extent there. In CON and TUR, the shallower mixed layers allow a better representation of the ice extent in this sector, with a slight overestimation in CON. Nevertheless, as already mentioned, the mixing can still be too intense in these two experiments, inducing low ice concentrations, as, for example, near 90°E. In experiment CON, one can notice a polynya near the Greenwich Meridian, a zone where such features have been commonly observed [e.g., *Comiso and Gordon*, 1987]. This region is also characterized by low ice concentrations in RI and TUR, but the ocean becomes completely ice free only in November. The causes and implications of this phenomenon will be analyzed thoroughly in a forthcoming paper. The maximum ice extent is overestimated in winter in the three experiments (Table 3). This problem has its major source in the Pacific sector of the Southern Ocean, where all simulations display roughly the same error (Figure 10). In experiment RI, the overestimation in the Pacific sector is compensated by an underestimation in the Indian sector, leading to a reasonable maximum ice extent. However, this compensation is not present in experiments TUR and CON, and thus the total ice extent appears too high.

In the Southern Ocean in spring and summer, the deeper mixed layers in CON and, to a lesser extent, in TUR (Figure 2) compared to RI are associated with higher heat fluxes at the ice base. For instance, the oceanic heat flux in the Weddell Sea averaged over the melt season (November-March) is 9.2 W m^{-2} in RI, 11.3 W m^{-2} in CON, and 10.7 W m^{-2} in TUR. The values during the freezing season (April-October) are closer to each other, with an average of about 28 W m^{-2} in the three experiments. To give an idea of the heat flux magnitude, a flux of 1 W m^{-2} during 6 months corresponds to a melting of 5 cm of ice. As a consequence, the minimum ice extent is lower in these two experiments than in RI (Table 3). Nevertheless, the

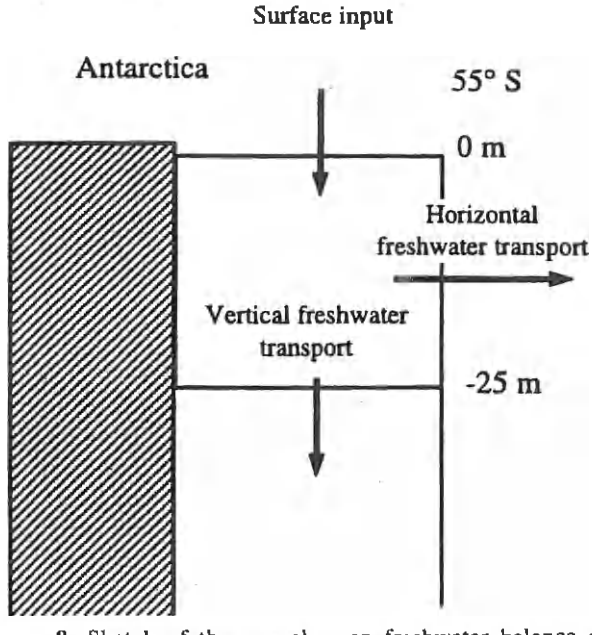

Figure 8. Sketch of the annual mean freshwater balance of the top 25 m of the ocean between 55°S and Antarctica. At equilibrium, the freshwater input at surface is balanced by the horizontal freshwater transport at the northern boundary and by the vertical freshwater transport to the deeper layers.

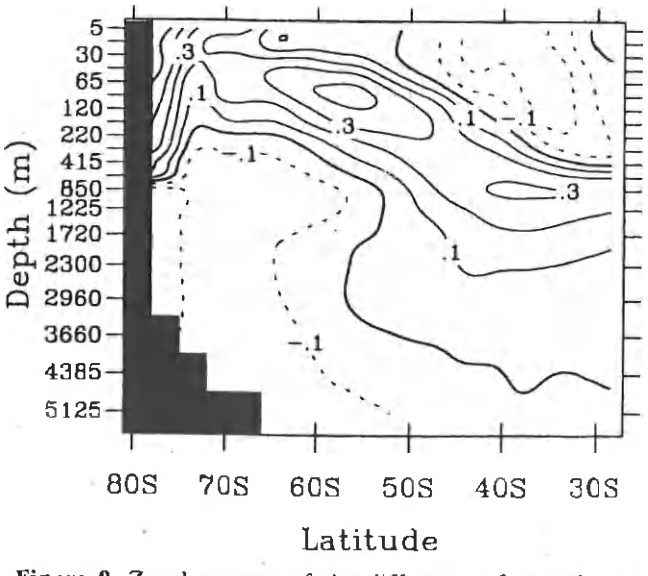

Figure 9. Zonal average of the difference of annual mean salinity between experiment TUR and *Levitus* [1982] data (TUR-Levitus). Contour interval 0.1 psu.

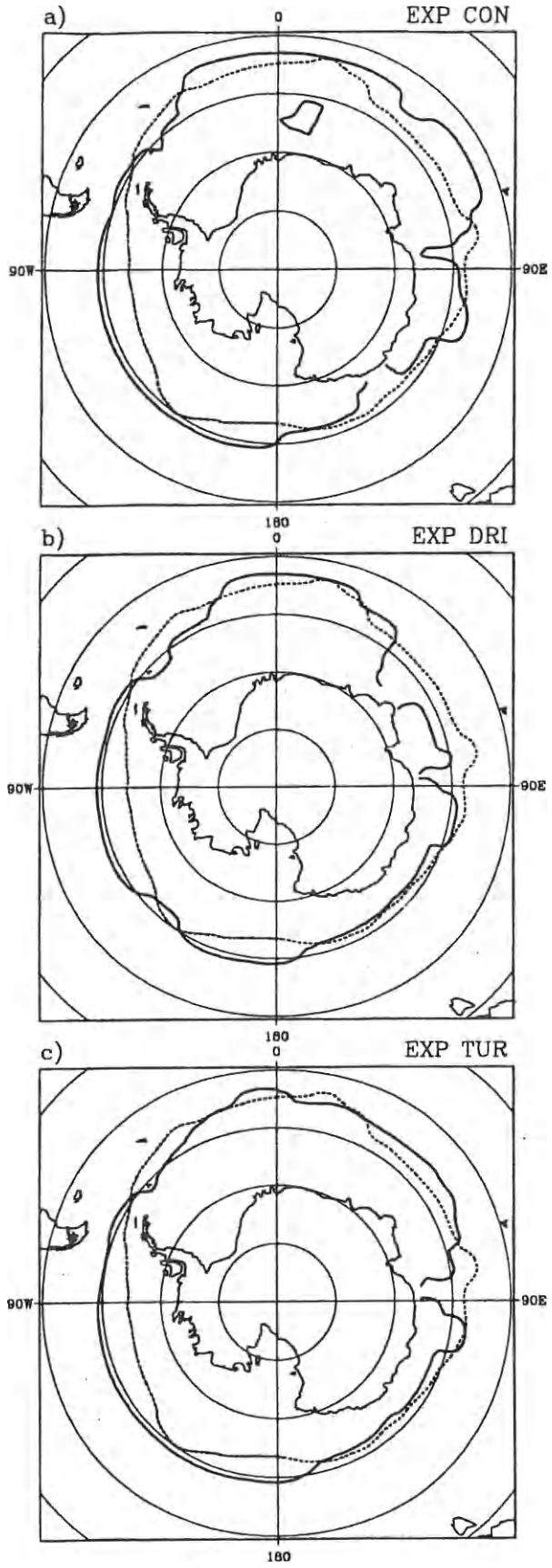

Figure 10. The position of the ice edge in the Southern Hemisphere (defined as the 15% ice concentration) simulated by the model (solid line) and observed (dashed line; *Gloersen et al.* [1992]) in September for experiments (a) CON, (b) DRI, and (c) TUR.

summer ice extent is overestimated in each experiment. This seems to be a common problem with models using the NCAR air temperature data [e.g., *Stössel et al.*, 1990; *Fichefet and Morales Maqueda*, 1997].

In the Northern Hemisphere, during winter, the mixed layer depths are only weakly affected by the parameterization of vertical mixing as is the oceanic heat flux at the ice base, and thus so too is the ice extent (Table 3). The only noticeable difference is a decrease of the ice extent in the Sea of Okhotsk of 0.3 x 10^{12} km^2 and 0.2 x 10^{12} km^2 in CON and TUR, respectively, compared to RI. This leads to a better representation of the ice concentration in these two experiments, although the ice extent is slightly overestimated in all the experiments (Figure 11). The cause of this decrease is the deeper summer mixed layers in TUR and CON, inducing a higher heat storage in the ocean which is used to limit the southward extension of the ice pack during winter. In summer, the MLD varies between the experiments, but it has only a very weak impact on the ice extent (Table 3). Indeed, the summer heat flux in the Arctic tends to be understimated in the three experiments with values generally lower than 1 W m^{-2} (compare with *Maykut and McPhee* [1995]). Therefore the modifications of this flux are not very important for the ice coverage there. A possible source of this flux underestimation and weak model sensitivy is our relatively coarse vertical resolution close to the surface, which is probably not sufficient to resolve the evolution of the shallow Arctic mixed layer [e.g., *Lemke and Manley*, 1984].

5. Summary and Conclusions

The sensitivity of a large-scale coupled ice-ocean model to the parameterization of vertical mixing in the upper ocean has been investigated. This has been achieved by comparing the results of three experiments. In the first one (CON), the wind-driven mixed layer is effectively assumed to have a constant depth of 50 m. In the second experiment, a slightly modified *Pacanowski and Philander* [1981] parameterization (PP81), which computes the vertical diffusivity and viscosity as a function of the local Richardson number, is applied. The third experiment (TUR) uses a simplified version of the Mellor and Yamada level 2.5 model [*Mellor and Yamada*, 1982; *Kantha and Clayson*, 1994].

It is found that the introduction of the turbulence scheme significantly improves the representation of the mixed layer depth as well as of the properties of the upper ocean, which is largely in agreement with other studies [see *Blanke and Delecluse*,1993; *Sterl and Kattenberg*, 1994; *Large et al.*, 1997]. The differences are particularly strong in summer. During this season, TUR gives reasonable results, although the MLD is a little shallower than observed. When using the PP81 parameterization (RI), the mixing in summer is strongly underestimated, with mixed layers shallower by 10-20 m compared to TUR. This is very significant because the mixed layer is generally between 20 and 50 m at this time. These spuriously shallow mixed layers are associated with an erroneously cold ocean at about 30 m, the surface warming not penetrating deep enough. However, the mixed layer is too deep in CON in summer (constantly at 50 m). Furthermore, the observed spatial distribution of the mixed layer is not at all reproduced in this experiment. This results in much too warm temperatures at about 50 m compared to observations. This problem might be reduced by using a more suitable depth for

Table 3. Maximum and Minimum Ice Extents in Both Hemispheres in the Three Experiments and in the Observations of *Gloersen et al.* [1992]

Experiment	Minimum in the Southern Hemisphere	Maxium in the Southern Hemisphere	Minimum in the Northern Hemisphere	Maxium in the Northern Hemisphere
CON	5.0	23.7	6.6	16.8
RI	6.5	20.4	6.6	17.2
TUR	5.6	22.0	6.6	16.9
OBS	3.8	18.8	9.2	15.8

Units are 10^{12} km^2.

the effective mixed layer but no value is valid globally and for all seasons. During winter, the mixed layer deepening in the model is mainly caused by a destabilizing surface buoyancy flux which generates relatively deep mixed layers. This process is parameterized by a standard convective adjustment in all three experiments, so the wintertime mixed layer depths are roughly the same, as are the temperatures and salinities of the winter mixed layer.

These results show that even with the classical limitations of OGCMs, a relatively sophisticated parameterization of vertical mixing provides a better representation of the evolution of MLD than simpler ones. The principal causes of the remaining deficiencies in TUR, such as the too shallow mixing in summer, are probably the use of monthly mean forcing and a too coarse vertical resolution. Indeed, various studies have demonstrated the importance of the atmospheric variability at short timescales as well as the need for a high resolution in the upper ocean to determine precisely the intensity of mixing in the ocean [e.g., *Miyakoda and Rosati*, 1984; *Rosati and Miyakoda*, 1988; *McPhee*, 1994]. In the future, we can expect that the problems will become less important because of improvement of model forcing and resolution. Presently, the atmospheric variability is already taken into account in OGCMs coupled to an atmospheric model or in some uncoupled OGCMs for studies performed on timescales of a few years. It is tempting, for comparison, to investigate if those model improvements would also affect experiments CON and RI. The answer is negative for CON since diffusivity is fixed. It is a little more complex for RI. Better forcing and resolution would probably improve the computation of the Richardson number. Nevertheless, there is no unique relationship between the Richardson number and the diffusivity [e.g., *Blanke and Delecluse*, 1993]. Therefore using equations similar to (3) and (4) would certainly pose problem in that case too.

The modifications of the MLD between the three experiments have an influence on heat exchange with the ice/atmosphere. The higher summer temperatures in CON are associated with a higher heat storage in the upper ocean. To feed this reservoir, the heat flux from the atmosphere into the ocean has to be higher. The difference between experiments TUR and CON can reach 50 W m^{-2} on a zonal mean. The heat reservoir is emptied during autumn when the mixed layer deepens again, leading to a higher heat flux from the ocean to the atmosphere in CON. The problem is opposite in RI, with too low a heat flux from the atmosphere to the ocean in summer because of the shallow mixed layer and too low a heat flux from the ocean to the atmosphere in autumn and winter.

Various studies have shown that the pycnocline and deep waters have their origin in the winter mixed layer, where our three experiments display only small differences. As a consequence, the ventilation of the intermediate and deep ocean is similar in experiments CON, RI, and TUR, with only marginal differences of temperature, salinity, and CFC concentration below 200 m. The only regions where significant changes occur in the deep levels are in the Southern Ocean. This particuliar behavior can be explained as follows. There the freshwater transport from the top 25 m to the layers below is higher in TUR and CON than in RI. The increase in CON is due to a higher freshwater flux at the surface associated with the salinity restoring and is thus not really physically based. However, the mechanism described in TUR is interesting. In this experiment, because of the higher vertical viscosities, the northward wind-induced transport in the upper ocean is distributed over a greater depth range than in RI or CON. As a consequence, the northward mass transport in the top 25 m is smaller in TUR and so therefore is the horizontal freshwater transport. In order to achieve the freshwater balance of the top 25 m, this must be compensated by an increase in the downward freshwater transport.

This higher vertical transport of freshwater in CON and TUR induces a decrease of the salinity between 25 and 100 m in these two experiments. This increases the stability of the water column and significantly reduces the pathological deep convection that is present in RI in the Southern Ocean. As a result, the ventilation of the Southern Ocean is slower. The shallower mixing in CON and TUR improves significantly the results in the Southern Ocean compared to RI. Nevertheless, the ventilation remains too strong, demonstrating that the problem also has other causes. A likely candidate is the simple representation of the effect of mesoscale eddies in our simulations [e.g., *England and Hirst*, 1997].

In RI, the heat brought from the deep ocean to the surface because of the strong vertical mixing in the Southern Ocean induces a significant underestimation of the ice extent, particularly in the Indian sector. The more reasonable MLD in TUR and CON allows a realistic winter ice extent in these two experiments. This illustates that complex interactions in the Southern Ocean, which include the effect of vertical viscosity, diffusivity, and freshwater transport, can have a significant impact on the ice cover. By contrast, in spring and summer, the mixed layer close to Antarctica in CON and TUR is deeper than in RI. This results in higher ice-ocean heat fluxes in these experiments and a decrease in the minimum ice extent of 30% in CON and 12% in TUR, compared to RI. In the Northern Hemisphere, the influence of the parameterization of vertical mixing is less important in our experiments, though it might be due to the coarse vertical resolution used in our study.

Vertical mixing parameterization is shown to be important in determining ocean ventilation, ice coverage, and ice-sea

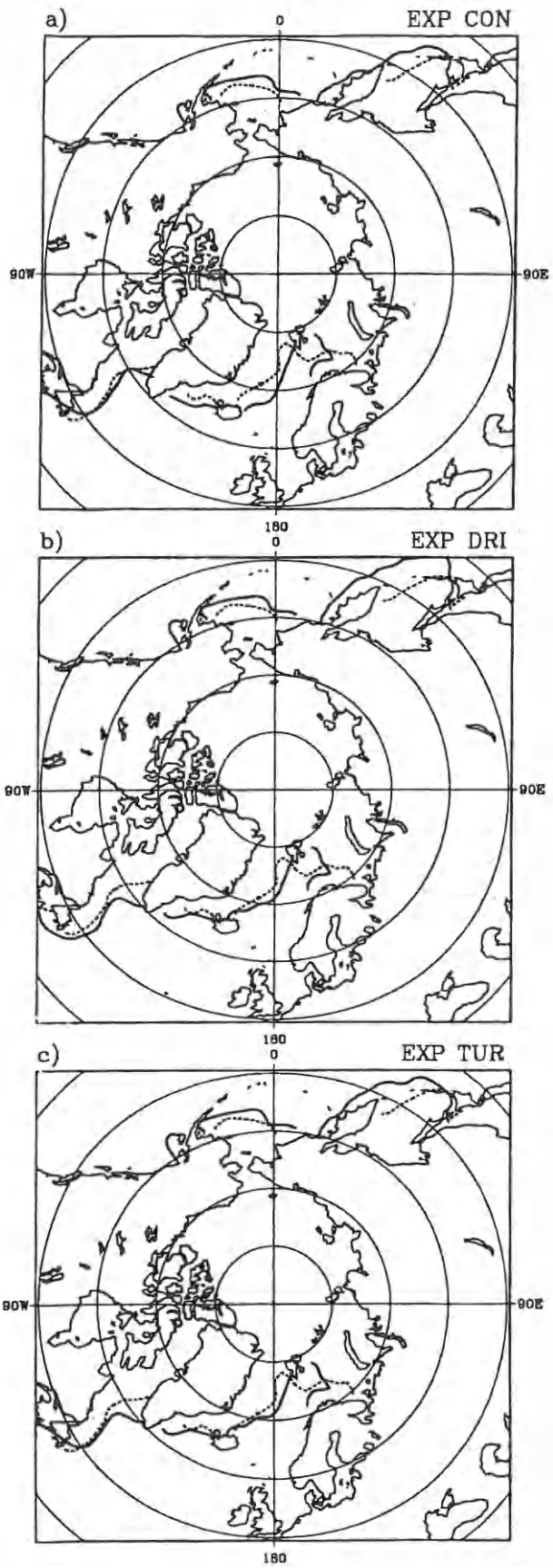

Figure 11. The position of the ice edge in the Northern Hemisphere (defined as the 15% ice concentration) simulated by the model (solid line) and observed (dashed line; *Gloersen et al.* [1992]) in March for experiments (a) CON, (b) DRI, and (c) TUR.

heat fluxes. It is difficult to assess precisely the effects on the atmosphere in the present framework, but it is certainly not negligible. For example, a correct simulation of ocean-atmosphere heat fluxes has been demonstrated to be critical to reduce the drift of coupled atmosphere-ocean models. Therefore great care should be taken to adopt a suitable mixing scheme in coupled climate studies. However, a sophisticated representation of vertical mixing in the upper ocean is probably less critical in ocean-only models devoted to the analysis of the long-term behaviour of the ocean interior since the effect of the various parameterizations is lower there. In such a case, an improvement of the representation of mixing below the surface layer or of the deep convection offers probably more opportunities.

Acknowledgments. We want to thank J.M. Campin, H. Cattle, A. Hirst, D. Martinson, and B. Tartinville for very interesting discussions about this work. The comments three anonymous reviewers were very much appreciated. H. Goosse, E. Deleersnijder, and T. Fichefet are sponsored by the National Fund for Scientific Research, Belgium. M. H. England acknowledges funding from the Australian Research Council and is indebted to the Université Catholique de Louvain for accommodating a visiting professorship during September - October 1997. This work was done within the scope of the Global Change and Sustainable Development Programme (Belgian State, Prime Minister's Services, Federal Office for Scientific, Technical, and Cultural Affairs, Contract CG/DD/09A), the Convention d'Actions de Recherche Concertées ARC 97/02-208 (Communauté Française de Belgique), and the Environment and Climate Programme (European Commission, Contract ENV4-CT95-0131). All these funding agencies are gratefully acknowledged.

References

Bathen, K.H., On the seasonal changes in the depth of the mixed layer in the North Pacific Ocean, *J. Geophys. Res.*, *77*, 7138–7150, 1972.

Baumgartner, A., and E. Reichel, *The World Water Balance*, 179 pp., Elsevier, New York, 1975.

Berliand, M.E., and T.G. Strokina, *Global Distribution of the Total Amount of Clouds* (in Russian), 71 pp., Hydrometeorological, Leningrad, Russia, 1980.

Blanke, B., and P. Delecluse, Variability of the tropical Atlantic Ocean simulated by a general circulation model with two different mixed-layer physics, *J. Phys. Oceanogr.*, *23*, 1363–1388, 1993.

Bleck, R., and L.T. Smith, A wind-driven isopycnic coordinate model of the north and equatorial Atlantic Ocean, 1, Model development and supporting experiments, *J. Geophys. Res.*, *95*, 3273–3285, 1990.

Bryan, F., Parameter sensitivity of primitive equation ocean general circulation models, *J. Phys. Oceanogr.*, *17*, 970-985, 1987.

Bryan, K., A numerical method for the study of the circulation of the world ocean, *J. Comput. Phys.*, *4*, 347–376, 1969.

Bryan, K., and L.J. Lewis, A water mass model of the world ocean, *J. Geophys. Res.*, *84*, 2503–2517, 1979.

Campin, J.-M., Modélisation tridimensionnelle de la circulation générale océanique lors du dernier maximum glaciaire, PhD thesis, Université Catholique de Louvain, Louvain-la-Neuve, Belgium, 1997.

Comiso, J.C., and A.L. Gordon, Recurring polynyas over the Cosmonaut Sea and the Maud Rise, *J. Geophys. Res.*, *92*, 2819–2833, 1987.

Crutcher, H.L., and J.M. Meserve, Selected level heights, temperatures and dew points for the Northern Hemisphere, *NAVAIR 50-1C-52*, revised, U.S. Naval Weather Serv., Washington, D.C., 1970.

Cubasch, U., G. Hegerl, A. Hellbach, H. Höck, U. Mikolajewicz, B.D. Santer, and R. Voss, A climate simulation starting in 1935, *Clim. Dyn.*, *11*, 71–84, 1995.

Da Silva, A.M., C.C. Young, and S. Levitus, Atlas of surface marine data 1994, vol. 1, Algorithms and procedures, *NOAA Atlas NESIDS 6*, 83 pp., U.S. Dep. of Commerce, Washington, D.C., 1994.

Deleersnijder, E., and J.-M. Campin, On the computation of the barotropic mode of a free-surface world ocean model, *Ann. Geophys.*, *13*, 675–688, 1995.

Deleersnijder, E., J.-P. van Ypersele, and J.-M. Campin, An orthogonal curvilinear coordinate system for a World Ocean model, *Ocean Modell.*, *100*, 7–10 (+figures), Hooke Inst., Oxford Univ., Oxford, England, 1993.

England, M.H., and A.C. Hirst, Chlorofluorocarbon uptake in a World Ocean model, 2, Sensitivity to surface thermohaline forcing and subsurface mixing parameterisations, *J. Geophys. Res.*, *102*, 15,709–15,731, 1997.

England, M.H., V. Garçon, and J.-F. Minster, Chlorofluorocarbon uptake in a World Ocean model, 1, Sensitivity to the surface gas forcing, *J. Geophys. Res.*, *99*, 25,215–25,233, 1994.

Fichefet, T., and M. A. Morales Maqueda, Sensitivity of a global sea ice model to the treatment of ice thermodynamics and dynamics, *J. Geophys. Res.*, *102*, 12,609–12,646, 1997.

Fichefet, T., H. Goosse, and M.A. Morales Maqueda, On the large-scale modeling of sea ice and sea ice–ocean interactions, in *Ocean Modeling and Parameterization*, edited by E.P. Chassignet and J. Verron, pp. 399-422, Kluwer Acad., Norwell, Mass., 1998.

Gloersen, P., W.J. Campbell, D.J. Cavalieri, J.C. Comiso, C.L. Parkinson, and H.J. Zwally, Arctic and Antarctic sea ice, 1978–1987: Satellite passive-microwave observations and analysis, *NASA Spec. Publ., SP-511*, 290 pp., Washington, D.C, 1992.

Goosse, H., Modelling the large-scale behaviour of the couped ocean–sea-ice system, Ph.D. thesis, 231 pp., Fac. des Sci. Appl., Univ. Cath. de Louvain, Louvain-la -Neuve, Belgium, 1997.

Goosse, H., J.-M. Campin, T. Fichefet, and E. Deleersnijder, Sensitivity of a global ice-ocean model to the Bering Strait throughflow, *Clim. Dyn.*, *13*, 349–358, 1997a.

Goosse, H., T. Fichefet, and J.-M. Campin, The effects of the water flow through the Canadian Archipelago in a global ice-ocean model, *Geophys. Res. Lett.*, *24*, 1507–1510, 1997b.

Hellerman, S., and M. Rosenstein, Normal monthly wind stress over the World Ocean with error estimates, *J. Phys. Oceanogr.*, *13*, 1093–1104, 1983.

Hibler, W.D., A dynamic thermodynamic sea ice model, *J. Phys. Oceanogr.*, *9*, 815–846, 1979.

Hirst, A.C., and W. Cai, Sensitivity of a world ocean GCM to changes in subsurface mixing parameterization, *J. Phys. Oceanogr.*, *24*, 1256–1279, 1994.

Hirst, A.C., and T.J. McDougall, Deep-water properties and surface buoyancy flux as simulated by a z-coordinate model including eddy-induced advection, *J. Phys. Oceanogr.*, *26*, 1320–1343, 1996.

Hsiung, J., Mean surface energy fluxes over the global ocean, *J. Geophys. Res.*, *91*, 10,585–10,606, 1986.

Hurlburt, H.E., and J.D. Thomson, Numerical study of Loop Current intrusions and eddy shielding, *J. Phys. Oceanogr.*, *10*, 1611–1651, 1980.

Iselin, C.O.D., The influence of vertical and lateral turbulence on the characterisics of water at mid-depths, *Trans. AGU*, *20*, 414–417, 1939.

Jaeger, L., Monatskarten des niederschlags für die ganze erde (in German), *Ber. Dtsch. Wetterdienstes*, *139*, 38 pp., 1976.

Johnson, E.S., and D.S. Luther, Mean zonal momentum balance in the upper and central equatorial Pacific Ocean, *J. Geophys. Res.*, *99*, 7689–7705, 1994.

Kantha, L.H., and C.A. Clayson, An improved mixed layer model for geophysical applications, *J. Geophys. Res.*, *99*, 25,235–25,266, 1994.

Lamb, P.J., On the mixed-layer climatology of the north and tropical Atlantic, *Tellus, Ser. A*, *36A*, 292–305, 1984.

Large, W.G., J.C. McWilliams, and S.C. Doney, Oceanic vertical mixing: A review and a model with a nonlocal boundary layer parameterization, *Rev. Geophys.*, *32*, 363–403, 1994.

Large, W.G., G. Danabasoglu, S.C. Doney, and J.C. McWilliams, Sensitivity to surface forcing and boundary layer mixing in a global ocean model: Annual-mean climatology, *J. Phys. Oceanogr.*, *27*, 2418–2447, 1997.

Latif, M., A. Sterl, E. Maier-Reimer, and M. Junge, Climate variability in a coupled GCM, I, The Tropical Pacific, *J. Clim.*, *6*, 5–21, 1993.

Latif, M., T. Stockdale, J. Wolff, G. Burgers, E. Maier-Reimer, M.M. Junge, K. Arpe, and L. Bengtsson, Climatology and variability in the ECHO coupled GCM, *Tellus, Ser. A*, *46A*, 351–366, 1994.

Lemke, P., and T.O. Manley, The seasonal variation of the mixed layer and the pycnocline under polar sea ice, *J. Geophys. Res.*, *89*, 6494–6504, 1984.

Levitus, S., Climatological atlas of the World Ocean, *Prof. Pap. 13*, 173 pp., Natl. Oceanic and Atmos. Admin., U.S. Dep. of Comm., Washington, D.C., 1982.

Manabe, S., and R.J. Stouffer, Multiple century response of a coupled ocean-atmopshere model to an increase of atmospheric carbon dioxide, *J. Clim.*, *7*, 5–23, 1994.

Maykut, G.A., and M.G. McPhee, Solar heating of the Arctic mixed layer, *J. Geophys. Res.*, *100*, 24,691-24,703, 1995.

McPhee, M.G., Turbulent heat flux in the upper ocean under sea ice, *J. Geophys. Res.*, *97*, 5365–5379, 1992.

McPhee, M.G., On the turbulent mixing length in the oceanic boundary layer, *J. Phys. Oceanogr.*, *24*, 2014-2031, 1994.

Meehl, G.A., A calculation of ocean heat storage and effective ocean surface layer depths for the Northern Hemisphere, *J. Phys. Oceanogr.*, *14*, 1747–1761, 1984.

Mellor, G.L., and T. Yamada, A hierarchy of turbulence closure models for planetary boundary layers, *J. Atmos. Sci.*, *31*, 1791–1806, 1974.

Mellor, G.L., and T. Yamada, Development of a turbulence closure model for geophysical fluid problems, *Rev. Geophys.*, *20*, 851–875, 1982.

Miyakoda, K., and A. Rosati, The variation of sea surface temperature in 1976 and 1977, 2, Simulation with mixed layer models, *J. Geophys. Res.*, *89*, 6533–6542, 1984.

Oberhüber, J.M., Simulation of the Atlantic circulation with a coupled sea ice-mixed layer-isopycnal general circulation model, I, Model description, *J. Phys. Oceanogr.*, *23*, 808-829, 1993.

Oey, L.-Y., and G.L. Mellor, Subtidal variability of estuarine outflow, plume, and coastal current: A model study, *J. Phys. Oceanogr.*, *23*, 164–171, 1993.

Oort, A.H., and T.H. Vonder Haar, On the observed annual cycle in the ocean-atmosphere heat balance over the Northern Hemisphere, *J. Phys. Oceanogr.*, *6*, 781–800, 1976.

Pacanowski, R.C., and S.G.H. Philander, Parameterization of vertical mixing in numerical models of tropical oceans, *J. Phys. Oceanogr.*, *11*, 1443–1451, 1981.

Philander, S.G.H. and R.C. Pacanowski, A model of the seasonal cycle in the tropical Atlantic Ocean, *J. Geophys. Res.*, *91*, 14,192-14,206, 1986.

Qiu, B., and R.X. Huang, Ventilation of the North Atlantic and North Pacific: Subduction versus obduction, *J. Phys. Oceanogr.*, *25*, 2374–2390, 1995.

Rosati, A., and K. Miyakoda, A general circulation model for upper ocean simulation, *J. Phys. Oceanogr.*, *18*, 1601–1626, 1988.

Sterl, A., and A. Kattenberg, Embedding a mixed layer model into an ocean general circulation model of the Atlantic: The importance of surface mixing for heat flux and temperature, *J. Geophys. Res.*, *99*, 14,139–14,157, 1994.

Stommel, H., Determination of watermass properties of water pumped down from the Ekman layer to the geostrophic flow below, *Proc. Natl. Acad. Sci. U.S.A.*, *76*, 3051-3055, 1979.

Stössel, A., P. Lemke, and W.B. Owens, Coupled sea ice-mixed layer simulations for the Southern Ocean, *J. Geophys. Res.*, *95*, 9539–9555, 1990.

Taljaard, J.J., H. van Loon, H.L. Crutcher, and R.L. Jenne, Climate of the upper air, I, Southern Hemisphere, Vol. I, Temperatures, dew points, and heights at selected pressure levels, *NAVAIR Rep. 50-1C-55*, 135 pp., U.S. Naval Weather Serv., Washington, D.C., 1969.

Trenberth, K.E., J.G. Olson, and W.G. Large, A global ocean wind stress climatology based on ECMWF analyses, *NCAR/TN-338 +STR*, 93 pp., Nat. Center for Atmos. Res., Boulder, Colo., 1989.

Wanninkhof, R., Relationship between wind speed and gas exchange over the ocean, *J. Geophys. Res.*, *97*, 7373–7382, 1992.

Washington, W.M., and G.A. Meehl, High-latitude climate change in a global coupled ocean-atmosphere-sea ice model with increased atmospheric CO_2, *J. Geophys. Res.*, *101*, 12,795–12,801, 1996.

Williams, R.G., M.A. Spall, and J.C. Marshall, Does Stommel's mixed layer "Demon" work ?, *J. Phys. Oceanogr.*, *25*, 3089–3102, 1995.

E. Deleersnijder, T. Fichefet, and H. Goosse, Institut d'Astronomie et de Géophysique G. Lemaître (ASTR), Université Catholique de Louvain, 2 Chemin du cyclotron, B-1348, Louvain-la-Neuve, Belgium. (hgs@astr.ucl.ac.be)

M. H. England, Centre for Environmental Modelling and Prediction (CEMAP), School of Mathematics, University of New South Wales, Sydney, NSW 2053, Australia.

(Received May 11, 1998; revised December 7, 1998; accepted March 19, 1999.)